Geophys. J. Int. (2004) **159,** 473–485 doi: 10.1111/j.1365-246X.2004.02393.x

Palaeomagnetic results from the Palaeozoic basement of the southern Drummond Basin, central Queensland, Australia

Kari L. Anderson,[1] Mark A. Lackie[2] and David A. Clark[3]

[1]*Department für Geo- und Umweltwissenschaften, Sektion Geophysik, Ludwig-Maximilians-Universität, Munich, Germany. E-mail: kari@geophysik.uni-muenchen.de*
[2]*Department of Earth and Planetary Sciences, Macquarie University, Sydney NSW* 2109, *Australia*
[3]*CSIRO Division of Exploration and Mining, North Ryde NSW* 2113, *Australia*

Accepted 2004 February 4. Received 2003 August 11; in original form 2002 September 2

SUMMARY

Palaeomagnetic results from the Theresa Creek Volcanics and the Middle Devonian (∼380 Ma) Retreat Batholith, located in the southern Drummond Basin, central Queensland, Australia, reveal up to three components of magnetization. Component 1 is characteristically of reversed polarity with a mean palaeopole at 64.0°S, 79.7°E ($N = 7$, $A_{95} = 11.5°$), possibly reflecting a remagnetization event associated with the Middle Carboniferous Alice Springs Orogeny, is found in both units. A shallow to very shallow roughly north–south direction, Component 2, was isolated in seven sites, predominantly within the Retreat Batholith, $D = 345.8°$, $I = -6.7°$ ($\alpha_{95} = 10.1°$, $k = 36.8$). The corresponding palaeomagnetic pole lies at 66.0°S, 290.7°E ($A_{95} = 9.1°$). This pole is consistent with the Middle Devonian segment of Australia's apparent polar wander path (APWP) and is thought to reflect a primary magnetization related to the emplacement and cooling of the batholith. Component 3 is found exclusively within the Theresa Creek Volcanics and is characterized by east–west directions with moderate to steep inclinations, $D = 62.4°$, $I = 59.5°$ ($\alpha_{95} = 10.5°$, $k = 25.0$). A consistent set of site level virtual geomagnetic pole (VGPs) yield a palaeopole at 4.1°N, 188.9°E ($N = 9$, $A_{95} = 14.0°$). The presumed Middle Devonian age for the volcanics is at odds with this direction, with respect to the Australian Early to Middle Palaeozoic APWP, suggesting the characteristic direction found in the volcanics reflects an Ordovician or possibly Early Silurian magnetization age. A pre-Middle Devonian magnetization age for the Theresa Creek Volcanics is supported by a positive contact test between the volcanics and the hornfelsing Retreat Batholith as both units are characterized by stable magnetizations whose palaeopoles are dissimilar from each other and younger segments of Australia's APWP.

Key words: APWP, Australia, Drummond Basin, palaeomagnetism, Palaeozoic.

1 INTRODUCTION

The Palaeozoic apparent polar wander path (APWP) for Australia since the Late Silurian is reasonably well constrained (e.g. Schmidt *et al.* 1987; Chen *et al.* 1993; Li & Powell 2001). The Ordovician–Silurian segment of the pole path, however, is plagued by a paucity of data and ambiguity concerning polarity, giving way to diverse palaeoreconstructions for the Early Palaeozoic (e.g. Li & Powell 2001; Torsvik & Rehnström 2001; Clark & Lackie 2003). Two sampling trips into the Drummond Basin (Fig. 1) were carried out, initially to study the palaeomagnetic response of the Middle Devonian Retreat Batholith (RB) and its contact aureole with the Theresa Creek Volcanics (TCV). Geochemical analyses presented by Deo (1991) and Withnall *et al.* (1995) had suggested that the TCV were cogenetic with the batholith and a late Early to Middle Devonian age was assigned to the hornfelsed volcanics. Results from a reconnaissance sampling trip in 1999 revealed a characteristic remanent magnetization (ChRM) associated with the TCV that was at odds with the Early to Middle Devonian age attributed to this formation. As preliminary palaeomagnetic data did not favour a temporal link between these two units, and geochronological data are not available for the TCV, a second excursion (in 2001) was designed to more fully incorporate a contact test between the TCV and RB in an effort to constrain the age of the TCV via palaeomagnetic techniques.

2 REGIONAL GEOLOGY

The Drummond Basin of central Queensland is an extensive backarc basin formed during the Late Devonian–Early Carboniferous, inboard of the New England Orogen (Davis & Henderson 1996). Basin development is largely attributed to backarc extension related to westward subduction (present-day coordinates) beneath the Late

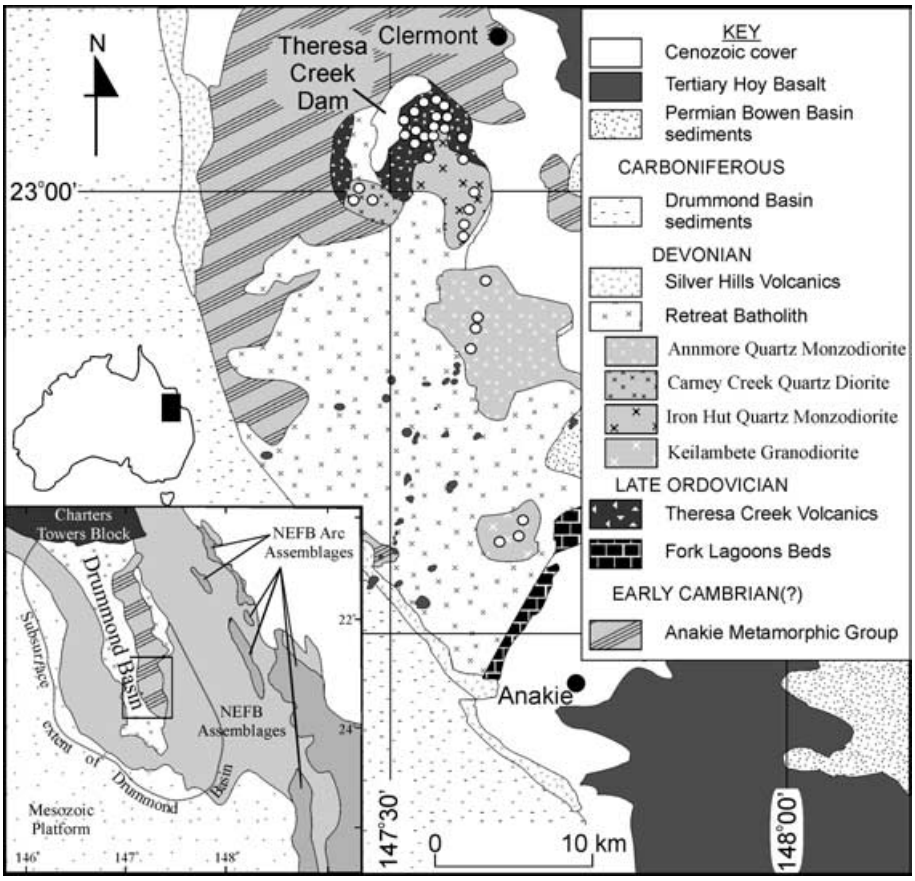

Figure 1. Simplified regional geology of the southern Drummond Basin, central Queensland, showing the relation of the Retreat Batholith and Theresa Creek Volcanics. Open circles represent sampling sites. The lower left inset shows the relation between the Drummond Basin and the Late Palaeozoic–Early Mesozoic New England Fold Belt (NEFB). Figure modified from Withnall *et al.* (1995).

Palaeozoic margin of Eastern Gondwana. Basement elements within the southern Drummond Basin include the Cambrian(?) Anakie Metamorphic Complex, the TCV and the RB (Fig. 1).

The RB (Fig. 1) is a large (∼1500 km^2) plutonic assemblage, comprising predominantly slightly mafic I-type granitoids. Rb–Sr and K–Ar dating of the batholithic assemblage has yielded ages of 366–385 Ma and 375–389 Ma, respectively, (Withnall *et al.* 1995). The Middle Devonian age of the RB indicates that it is at least partly contemporaneous with the Ordovician–Devonian Calliope Island Arc of eastern Australia, suggesting that the batholith may have been emplaced in a backarc setting. Geochemical analyses presented by Withnall *et al.* (1995) support an arc-related origin for the RB, as data fall within syncollisional granitoids and volcanic-arc granitoid fields on plots of Rb versus Y + Nb and Nb versus Y. However, it has also been proposed (Veevers *et al.* 1982; Powell 1984) that a more probable tectonic origin for the batholith is one similar to that of the Basin and Range Province of western North America. Plutons associated with the RB intrude the pre-Ordovician Anakie Metamorphic Group, the TCV and the Ordovician Fork Lagoons Beds; the plutons are disconformably overlain by the Devonian–Carboniferous Silver Hills Volcanics. Palaeomagnetic results for the Silver Hills Volcanics were presented by Klootwijk *et al.* (1993).

The environment of deposition of the TCV is thought to have been largely subaerial; no pillow lavas or well-bedded sedimentary rocks are associated with the volcanics, but its tectonic origin is uncertain (Withnall *et al.* 1995). Lithologically, the TCV is characterized by flat-lying andesites and mafic lavas, with fewer occasional breccias and volcanolithic arenites. The age of the TCV is poorly constrained. There are no radiometric data and no fossils within the TCV, and mapping of relationships in the region is hampered by widespread Cenozoic cover. The only definitive conclusion about the relative position of the TCV is that it overlies metamorphics belonging to the pre-Ordovician Anakie Group and is intruded by the RB (Withnall *et al.* 1995). A Middle Devonian age had been assigned to the TCV, based largely upon a geochemical similarity between the TCV and granites associated with the RB (e.g. Deo 1991; Withnall *et al.* 1995). However, it has also been suggested (G. Brock, personal communication, 2001) that the Emsian Douglas Creek Limestone overlies the TCV, suggesting a minimum age of Early Devonian for the TCV. There are Late Ordovician (Bolindian) volcanics and volcaniclastic sediments in the southern Drummond Basin, the continental-arc-related Fork Lagoons Beds, with which the TCV might be correlative (I. Withnall, personal communication, 2002; P. Blake, personal communication, 2002).

3 FIELD METHODS AND LABORATORY TECHNIQUES

Six of the 19 sampled sites within the TCV were along the southern margin of the volcanics, an area hornfelsed by a pluton associated with the RB. A total of 17 sites were sampled from RB plutons to establish a contact test (Everitt & Clegg 1962) between the TCV and the younger granites. Both block samples and palaeomagnetic

drill core (three to seven per site) were collected in the field and all samples were oriented using both sun and magnetic compasses. Exposure within this region is fair to poor, as both the TCV and granites within the RB tend to weather quickly, and sampling was, therefore, preferentially conducted within gullies and creek beds in an effort to obtain the freshest possible samples. Samples collected at all sites were taken several metres apart in an effort to minimize the effects of any lightening-induced remanence (LIRM) affecting the site or to aid in recognition of LIRM. All sites were separated by a minimum of 200 m.

In the laboratory, block samples were reoriented, and two to four 2.5 cm diameter cores were taken from each block. All cores were sliced into one to four specimens, 2.2 cm in height. Prior to demagnetization procedures, bulk susceptibilities were measured for all specimens. For nearly all specimens, intensities and directions of the natural remanent magnetization (NRM) were determined using a horizontally mounted 2G755R d.c. SQUID magnetometer in the rock magnetism laboratory at the Commonwealth Scientific and Industrial Research Organisation (CSIRO), Sydney. NRM intensities from two sites in the TCV, TCV01 and TCV12, were in excess of the operational sensitivity of the cryogenic magnetometer and were measured using a Digico fluxgate spinner magnetometer interfaced to a PC at CSIRO. Following the initial NRM measurement, at least two specimens per sample were treated with low-temperature demagnetization, cooling of the specimens in liquid nitrogen and rewarming to room temperature in zero field (LN_2 step). Low-temperature demagnetization was used to reduce magnetizations carried by multidomain magnetite or LIRM (Schmidt 1993). Following the LN_2 step, specimens were treated with standard step-wise thermal and/or alternating field (AF) demagnetization, up to maximum temperatures and fields of 700 °C and 160 mT, respectively.

Demagnetization behaviour was monitored throughout via orthogonal vector diagrams (Zijderveld 1967) and equal-area stereographic projections. Principal component analysis (PCA) (Kirschvink 1980) was the primary method used to determine characteristic and secondary magnetization components, and when linear segments of demagnetization vectors could be identified site-mean directions were calculated according to standard methods (Fisher 1953). At times, complex magnetization histories were observed within the TCV and RB, prompting the incorporation of remagnetization circles with direct endpoint observations (McFadden & McElhinny 1988) in an attempt to better define characteristic directions. Filtering of palaeomagnetic data consisted of rejecting samples lacking between-specimen consistency and also specimens for which components had maximum angular deviation (MAD) of $>15°$, or those displaying chaotic behaviour. Additionally, data were discarded from sites with fewer than three remaining samples. Specimen-level data were averaged into a sample mean. Site-level virtual geomagnetic poles (VGPs) were calculated when minimum-filtering criteria had been met and were used in the computation of mean palaeopoles.

Demagnetization behaviour and the results of rock magnetic tests, including hysteresis curves, coercivity spectra, isothermal remanent magnetization (IRM), thermal demagnetization of saturation magnetization (J_s–T) and thermal demagnetization of three-component isothermal remanent magnetization (3D-IRM), were analysed to determine mineralogy and structure of remanence carriers within the TCV and RB. A Petersen variable field translation balance (VFTB), manufactured by the University of Munich, was used to conduct J_s–T, IRM, coercivity spectra and hysteresis curve experiments. For imparting 3D-IRM (Lowrie 1990), the following fields were applied to each specimen: 1 T along the z-axis, 0.1 T along the y-axis and 0.01 T along the x-axis.

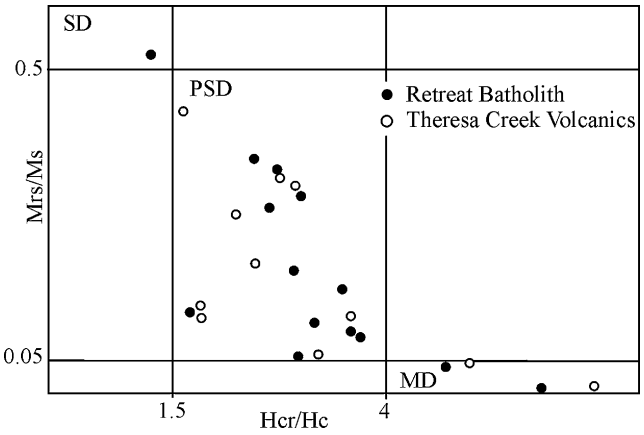

Figure 2. Day plot (Day *et al.* 1977) of magnetite remanence carries for the Retreat Batholith and Theresa Creek Volcanics.

Geochemical data available in Withnall *et al.* (1995) were used to determine if a genetic similarity between the TCV and basalts associated with the Fork Lagoons Beds existed. Results from this analysis are discussed below.

4 RESULTS

4.1 Rock magnetic results

Palaeomagnetic tests indicate unblocking temperatures (T_{ub}) for most TCV and RB sites were generally between 500 and 580 °C and median destructive fields were less than 60 mT. Demagnetization results and VFTB investigations identified pseudo-single-domain (PSD) magnetite as the dominant remanence carrier for both formations. Hysteresis and backfield coercivity data were used to generate Day plots (Day *et al.* 1977) for magnetite series carriers, shown in Fig. 2. The trend from single-domain (SD) through PSD to multidomain (MD) fields within the Day plot reflects the fine to coarse grain size mixture of magnetites (Dunlop & Özdemir 1997) within the RB and TCV. Figs 3(a) and (b) show typical responses from the RB and TCV during high-field demagnetization (J_s–T) tests, confirming the presence of magnetite with unblocking temperatures between 550 and 580 °C. The near-perfect reversibility seen in J_s–T curves after heating to 700 °C suggests that the magnetite within the RB and TCV is not due to mineralogical alteration resulting from heating and that the magnetite is inert to such heating. Demagnetization spectra of the 3D-IRM for the RB and most TCV sites, Figs 3(d) and (e), also indicate that the medium-coercivity spectra (magnetite) are dominant, as expected from related rock magnetic data obtained from the VFTB.

Within the hornfelsed zone of the TCV, haematite is the characteristic remanence carrier, as identified via unblocking temperatures of palaeomagnetic components, J_s–T and 3D-IRM data, combined with data from backfield coercivity and standard IRM tests. Typical results for the hornfelsed TCV samples include backfield coercivity values generally in excess of 80 mT and unsaturated IRM curves in maximum laboratory fields (∼0.78 T). Fig. 4 shows IRM and backfield coercivity data from three sites within the zone of contact between the TCV and RB. Not all sites within this region are included in this representative diagram, as highly variable magnetic intensities across the contact zone precluded a meaningful display

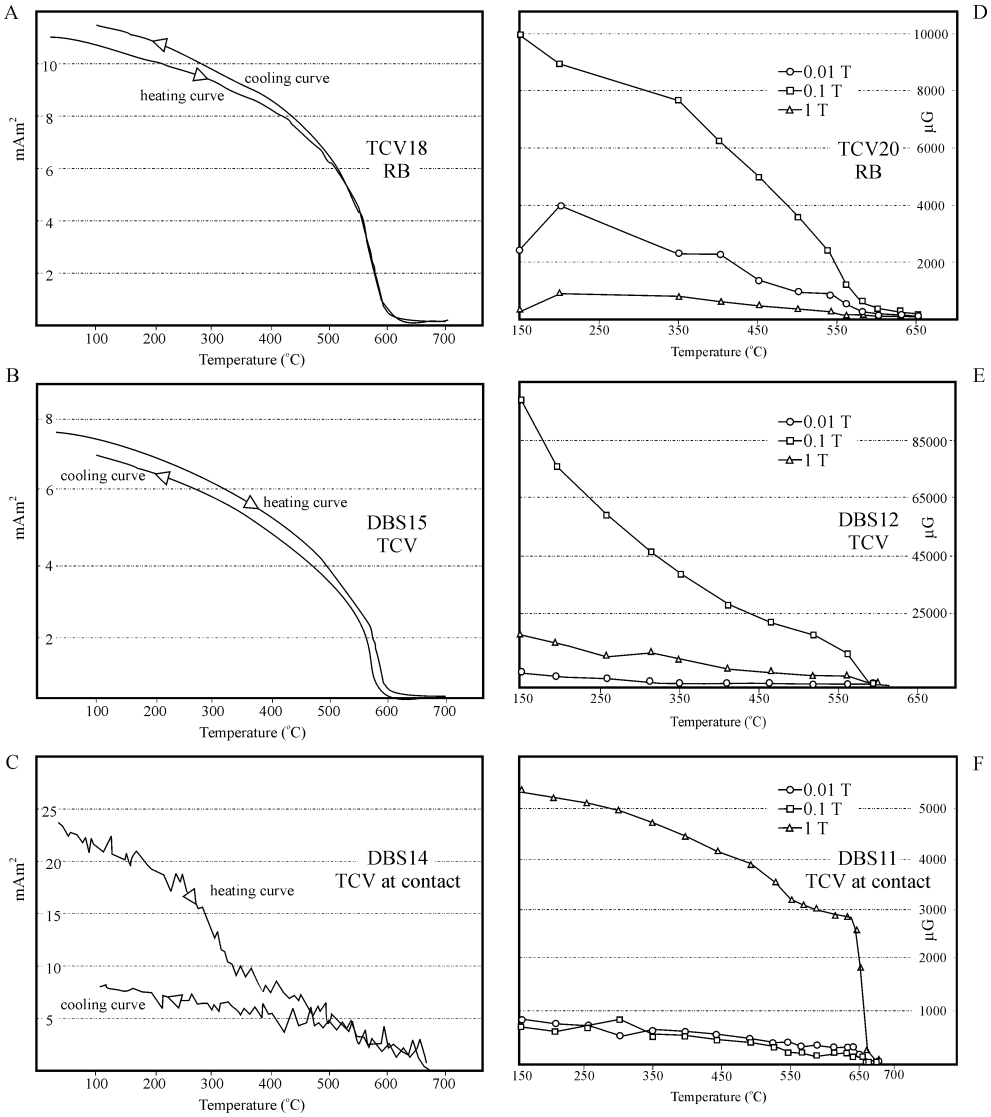

Figure 3. Panels (A)–(C) show J_s–T results from the RB, TCV and hornfelsed TCV. Panels (D)–(F) are representative 3D-IRM plots. Magnetite is dominant in the results presented in (A), (B), (D) and (E). Results from the hornfelsed TCV reflect a large haematite contribution (C, F).

of these data. Unblocking temperatures of ∼680 °C, evident from J_s–T tests (Fig. 3c), and dominance of the hard coercivity component in thermal demagnetization of 3D-IRM (Fig. 3f) support the identification of haematite as the principal remanence carrier within the hornfelsed volcanics.

4.2 Geochemical analysis

To the south of the Theresa Creek Dam area lie the Late Ordovician (Bolindian; Cook & Totterdel 1991) Fork Lagoons Beds (FLB), comprising limestones, mudstones and mafic volcanics (Fig. 1). The relation of the FLB to the underlying Anakie Metamorphic Group is uncertain, much like that of the TCV, and the FLB are likewise hornfelsed by plutons of the RB. Fig. 5 shows a spider diagram of geochemical data available from the TCV and FLB, taken from Withnall *et al.* (1995). Normalized isotope values were computed using the carbonaceous chondrite composition of McDonough & Sun (1995).

Using the available geochemical data on these two formations (Fig. 5) it is not possible to fully substantiate their cogenetic origin, as the available data document only that the TCV are more evolved than the basalts related to the FLB. It is unclear whether this is a reflection of some degree of fractional crystallization within a shared magma source or merely a coincidental outcome based upon analysed rock type. At this stage, however, a genetic and temporal link between these two suites of volcanics cannot be excluded and, based upon palaeomagnetic data (discussed below) and the lack of convincing structural, radiometric or geochemical data that show otherwise, a Late Ordovician–Early Silurian age for the TCV is favoured.

4.3 Great circle analysis

Twenty-six of the total of 102 samples from the TCV and RB judged suitable for palaeomagnetic analyses did not allow the isolation of a ChRM during AF demagnetization. Instead, the AF demagnetization of these samples results in a series of magnetization vectors that were generally coplanar, forming remagnetization circles during progressive demagnetization. These remagnetization circles trend toward ChRMs determined from sister samples that were thermally

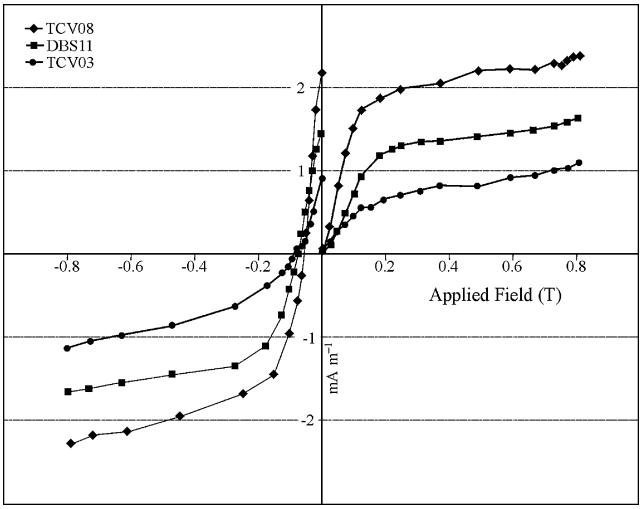

Figure 4. Representative IRM and backfield coercivity data from the hornfelsed TCV.

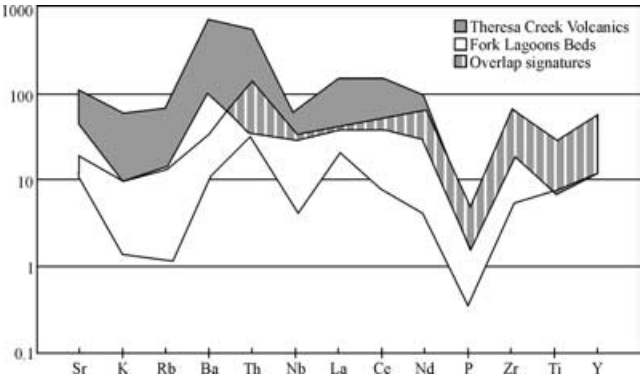

Figure 5. Spider diagram of the TCV and Fork Lagoons Beds using normalized Carbonaceous chondrite composition values of McDonough & Sun (1995).

treated, reflecting the overlapping spectra of two coercivities. Combination of remagnetization circles with the ChRMs (set points) from other samples within a given site was used to constrain the direction of the characteristic component during great circle analysis (GCA) (McFadden & McElhinny 1988). Data from neighbouring sites that revealed similar magnetization components (defined solely by sample-level ChRMs) were used to apply sector constraints (McFadden & McElhinny 1988) on those samples that were characterized by remagnetization circles. The potential bias in the GCA method, discussed by Schmidt (1985), is not thought to be significant within this study for the following reasons: one or more set points were available from each site in which GCA was applied; tight sector constraints were employed for all GCA analyses; and none of the resultant components were defined solely by the GCA method. As a consistency check, however, the resultant southern Drummond Basin palaeomagnetic data, presented in Table 1, were calculated with and without the inclusion of GCA data.

4.4 Palaeomagnetic results and interpretations

Although homogeneous on the site level, intensities of the NRM were variable for the TCV and RB granites, with site-level median values ranging between 40 and 2000 mA m^{-1}. Wide scatter in NRM directions and Koenigsberger ratios for most specimens of less than 0.1 attest to the existence of multiple magnetization components within these units. Following the removal of a viscous present field direction with low unblocking temperatures/fields ($\leq$350 °C/20 mT), either linear decay of magnetization vectors or remagnetization circles revealed up to three ChRM directions within the TCV and RB granites, all having moderate to high unblocking temperatures and fields.

Component 1 (C1) within the TCV and RB is characteristically south with moderate down inclination directions. A very shallow north–south component (C2) was found in sites associated with the RB and as scattered sample-level ChRMs within the TCV. A third dual-polarity component (C3) was identified exclusively within the TCV. All components were determined by either standard PCA methods (Kirschvink 1980) or incorporation of remagnetization circles in a GCA (McFadden & McElhinny 1988). The angular dispersion (S) of each set of VGPs, when compared with the appropriate palaeolatitude, is concordant with analyses of palaeosecular variation during the past 5 Myr (Butler 1992), suggesting that secular variation has been adequately averaged. Representative demagnetization data are shown in Fig. 6. Typical site-level remagnetization circles and set-point plots are displayed in Fig. 7. Remanence directions are discussed in detail below and all palaeomagnetic data are presented in Table 1.

Component 1

C1/1′ is of dual polarity (C1/1′ represent the reverse/normal magnetization populations, respectively) and is found in 12 sites (53 samples) within both the TCV (nine sites) and the RB (three sites). The mean direction of C1/1′ is $D = 199.2°$, $I = 45.7°$, $k = 29.8$, $\alpha_{95} = 8.1°$. Although the antipode of C1 is dissimilar from the present day field at the 95 per cent confidence interval, the normal polarity component, C1′, cannot be distinguished from the present field at this level. Because of the very stable palaeomagnetic behaviour observed for C1′ (coercivities of remanence up to 60 mT and $T_{ub} \geq 500$ °C) it is thought that rather than solely reflecting a persistent present or Recent field magnetization, the proximity of C1′ and present field directions is the result of an inability to fully remove a secondary component, perhaps acquired during sustained Tertiary weathering. This is borne out by analytical observations, including: a non-Fisherian distribution of C1′; site-level C1′ directions streaking between the expected present field direction and the C1 antipode; the small degree of arc separating the C1′ component and present field (11.3°); and the reverse polarity component, C1, being readily identifiable without incorporating GCA to the extent necessary for the normal polarity directions. Fig. 8(a) shows the site-level mean directions of C1/1′, including the relation of C1′ with the present field direction expected within the sampling region. A site parametric bootstrap reversal tests shows that C1/1′ cannot be distinguished at the 95 per cent confidence interval (Tauxe 1998). The probable contamination of C1′ by a Recent weathering-related remagnetization, however, suggests that the reverse polarity C1 direction ($D = 208.1°$, $I = 47.8°$, $k = 29.0$, $\alpha_{95} = 11.4°$) more truly reflects the characteristic magnetization for this direction. The mean palaeopole direction obtained using only C1 sites lies at 64.0°S, 79.7°E ($N = 7$, $A_{95} = 11.5°$).

Component 2

C2 directions were isolated in the Keilambete Granodiorite, Annmore Quartz Monzodiorite and Iron Hut Quartz Monzodiorite plutons of the batholith (Fig. 1). C2 has north–south directions with

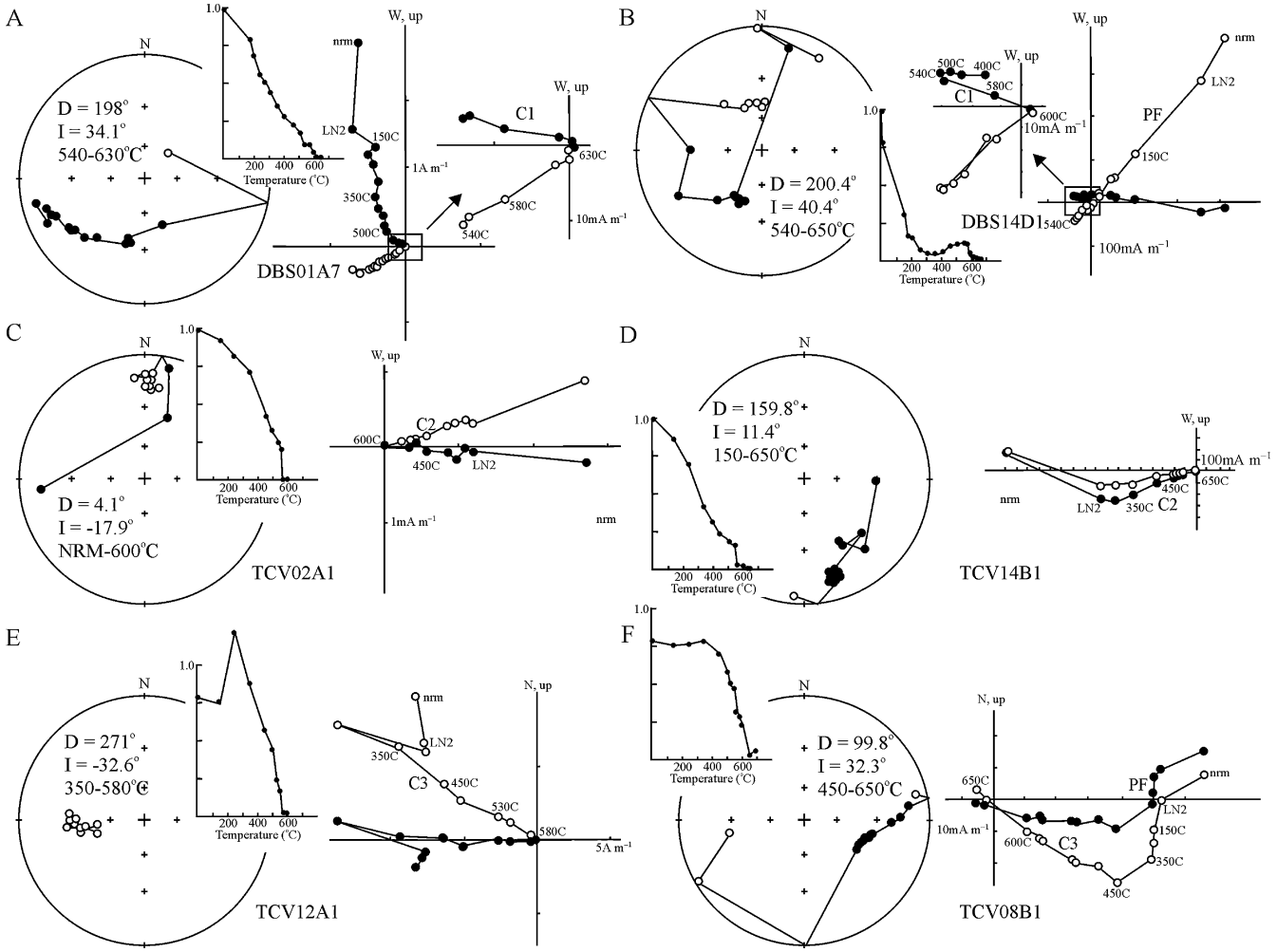

Figure 6. Demagnetization data for the TCV and RB. Stereonets are equal-area projections in which the open/closed circles represent upper/lower hemisphere projections. Open/closed circles in the orthogonal vector diagrams represent vertical/horizontal projections. PF (present field), C1, C2 and C3 components are labelled on each vector plot and directions are given for each sample.

shallow to very shallow inclinations. In five of the 17 RB sites, 17 of 58 samples, C2 was obtained either directly as a ChRM direction or as information available from remagnetization circles (McFadden & McElhinny 1988). Of the remaining 12 sites sampled within the RB, four sites within the Iron Hut Quartz Monzodiorite (Fig. 1a) have retained the C2 direction, but only in one or two samples per site, with other samples from these sites not yielding coherent palaeomagnetic results. These data have been combined into the DGH composite direction ($n = 8$) in Table 1. Conformity of palaeomagnetic data from the these plutons suggests that the constituent members of the RB have not been significantly tilted as a consequence of emplacement or later deformation. Seven sites from the RB failed to give meaningful palaeomagnetic results, while one site, from the Carney Creek Quartz Diorite, carried only the C1 direction discussed above.

The C2 remanence direction was also recognized in a few scattered TCV samples ($n = 9$) coming from the contact zone between the TCV and RB where it is thought to reflect a thermal remagnetization and haematization of the hornfelsed volcanics. As this direction could not be isolated on the site level within the volcanics, data were incorporated into a single temporal 'site', TCV-2 in Table 1, for inclusion in subsequent analyses.

Unblocking temperatures and median destructive fields for C2 were high for the granites (560–580 °C, 55–80 mT) and within the TCV unblocking temperatures were in excess of 630 °C. Small sample populations of the normal and reverse directions, together with dissimilar dispersion values, encouraged the use of a parametric bootstrap reversal test for this component (Tauxe 1998; McElhinny & McFadden 2000) and at the 95 per cent confidence interval, inverted northern directions cannot be distinguished from their southern antipodes. The mean ChRM for C2, using data from 34 samples (seven sites) is $D = 345.8°$, $I = -6.7°$ ($k = 36.8$, $\alpha_{95} = 10.1°$), Fig. 8(b). The corresponding palaeopole lies at 66.0°S, 290.7°E, $A_{95} = 9.1°$.

Component 3

C3, a dual polarity, east–west direction with moderate to steep inclinations, is seen only within the TCV and then only at distances greater than 1 km from the contact between the TCV and the Iron Hut Quartz Monzodiorite pluton of the RB (see Fig. 1). C3 is found in 37 samples from nine sites within the TCV as either ChRM or remagnetization circles and is isolated at temperatures and fields in excess of 500 °C and 50 mT, respectively. The mean direction of

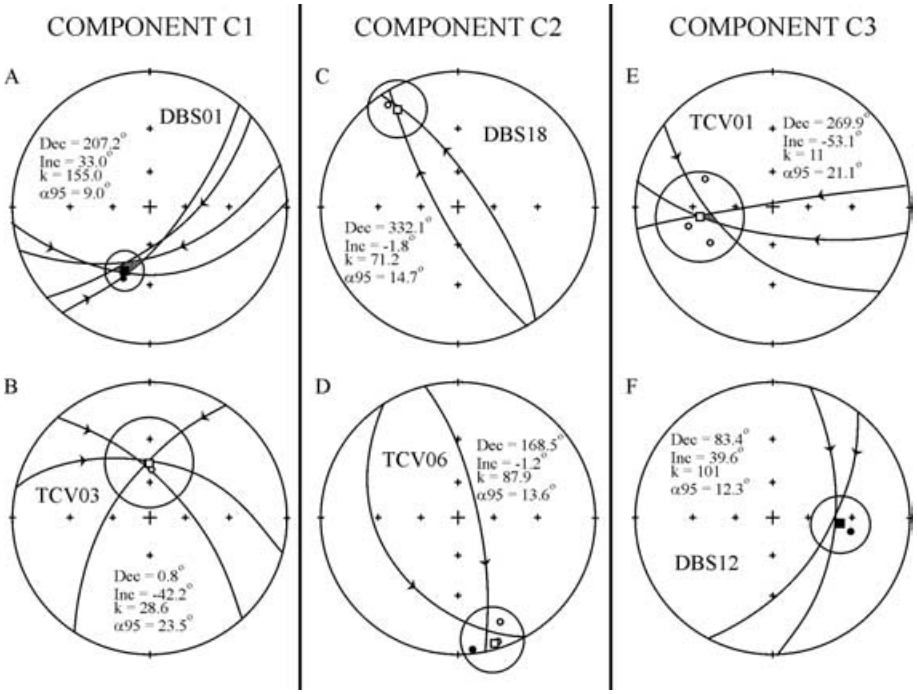

Figure 7. Great circle analysis data for each of the three components. Shaded regions in (A), (B) and (E) represent the area on the stereonet in which the remagnetization circles intersect. All plots are equal-area projections. (A) and (F) are lower hemisphere projections while (B)–(E) show upper hemisphere data. Statistics were calculated as outlined by McFadden & McElhinny (1988).

site-level ChRMs is $D = 62.4°$, $I = 59.5°$ ($N = 9, \alpha_{95} = 10.5°, k = 25.0$), Fig. 8(c). When the mean for normal polarity sites is inverted to its reverse antipode, reverse and normal directions cannot be distinguished at the 95 per cent confidence interval using the bootstrap reversal test of Tauxe (1998). The corresponding nine VGPs yield a mean palaeopole at 4.1°N, 188.9°E, $A_{95} = 14.0°$, Table 1.

The presumed Middle Devonian age for the TCV (Withnall *et al.* 1995) is at odds with the palaeopole calculated from the C3 direction, with respect to the Australian APWP. As the TCV lacks a definitive radiometric age and the relative age of the unit is only constrained by the pre-Early Ordovician Anakie Metamorphic Group and the Middle Devonian RB, determining the age of the TCV via palaeomagnetic techniques is a viable alternative. In the APWP presented in Fig. 9, the location of the TCV palaeopole allows at least three possible scenarios:

(1) This direction reflects a younger overprinting event of unknown age and anomalous direction.

(2) The volcanics are tilted, possibly as a result of batholithic emplacement and/or a tectonic rotation displacing the observed palaeopole away from Australia's APWP.

(3) The TCV are Ordovician or Early Silurian in age.

Whilst the first option remains a possibility, it is unlikely given our present understanding of the Palaeozoic and younger APWP for Australia, and the failure to find this direction within the batholith or the contact zone between the RB and TCV. If C3 were the result of a younger magnetization event, one would expect it to have had a regional affect within the southern Drummond Basin and not be concentrated within a single formation, similar to the distribution of the C1 direction.

Structural information available from the southern Drummond Basin essentially precludes a tectonic rotation (Withnall *et al.* 1995) and bedding attitudes for the TCV were largely subhorizontal. Indeed, short of rotating the Anakie Inlier as an entity sometime during the Early Palaeozoic, but before the Middle Devonian, a tectonic correction for the C3 palaeopole cannot be supported based upon available field data (Withnall, personal communication, 2002), leaving open the possibility that the TCV are substantially older than had previously been thought.

5 DISCUSSION

Of the three ChRMs revealed during the investigation of the southern Drummond Basin, only C2, from the RB, is well dated with a magnetization age corresponding to a known formation age. Although of a limited population, C2 is considered to reflect a primary thermochemical magnetization for the RB. Using the quality criteria of (Van der Voo 1990), with the positive result of the contact test (Everitt & Clegg 1962) between the RB and TCV, the RB palaeopole has a $Q = 7$. The corresponding palaeopole (RB in Fig. 9) falls between the Late Devonian Worange Point (WP) (Thrupp *et al.* 1991) and the Early Devonian Snowy River Volcanics (SRV) (Schmidt *et al.* 1987) palaeopoles for Australia's APWP, WP and SRV, respectively, in Fig. 9. Fixing the APWP to both the RB and the high-quality SRV (Schmidt *et al.* 1987) poles (Fig. 9) introduces a nearly symmetric set of cusps into this segment of the APWP. The two changes in plate motion represented by these swings in the Late Silurian–Early Devonian segment of the presented APWP may perhaps be reflections of far-field effects of interactions between Western Gondwana and the Laurussian continent during the Caledonian Orogeny (Schmidt & Embleton 1990). (All palaeopoles used in the construction of the APWP in Fig. 9 are presented in Table 2.)

The C1 direction is likely to be a reflection of the effects of the Middle Carboniferous Alice Springs Orogeny (ASO) as recorded by units in the southern Drummond Basin. In recent years, protracted continent-wide deformation related to the ASO has been

Table 1. Palaeomagnetic components from the Drummond Basin.

Component 1															
Site	FM	Slat (°S)	Slong (°E)	Dec (°)	Inc (°)	*n*/*N*	*n*/*C*	*R*	*k*	α_{95}(°)	*s* (°)	λ (°N)	ϕ (°E)	*dp* (°)	*dm* (°)
DBS18	RB	23.4326	147.6259	211.0	64.8	3/5		3.0	385.5	8.7	4.1	−56	108.5	11.3	14.9
TCV24	RB	22.9263	147.5307	193.8	43.6	6/7		6.0	132.9	6.5	7.0	−77.2	71.7	5.1	8.1
DBS02	RB	22.9909	147.4728	213.2	49.7	5/5		4.8	19.5	17.8	18.3	−59.5	79	15.8	23.7
DBS01	TCV	22.9243	147.5321	207.2	33.0	5/5	1/4	5.0	155.0	9.0	6.5	−64.1	51.6	5.8	10.2
DBS11	TCV	22.9215	147.5438	209.8	63.2	7/7		6.7	20.8	13.5	17.8	−57.4	106.6	16.8	21.1
DBS13	TCV	22.9331	147.5201	226.0	33.3	5/5		4.8	24.4	15.5	16.4	−46.8	60.1	10.0	17.6
TCV01	TCV	22.9086	147.5609	195.7	43.4	3/7		3.0	72.3	14.6	9.5	−75.5	69.9	11.3	18.1
DBS12	TCV	22.9245	147.5337	17.2	−45.7	6/7		5.8	22.4	14.5	17.1	−73.9	76.2	11.8	18.5
DBS16	TCV	22.9263	147.5481	24.1	−42.4	3/5		3.0	46.6	18.3	11.9	−67.9	66.6	13.9	22.5
TCV03	TCV	22.9606	147.5457	0.8	−42.2	4/5	1/3	3.9	49.2	14.2	12.4	−88.4	120.5	10.8	17.5
TCV09	TCV	22.9197	147.5556	4.3	−42.0	4/5	2/2	3.9	21.2	20.4	17.6	−85.5	76.9	15.3	25.0
TCV10	TCV	22.9206	147.5581	356.1	−34.0	3/5		3.0	48.1	18.0	11.7	−84.4	286.4	11.8	20.6
		λ	ϕ	A_{95}		*D*	*I*	*N*	*k*						*Q*
ChRMs		68.7°S	80.8°E	10.5°		202.2°	47.6°	9	28.5						
C1/1′		71.7°S	77.6°E	8.8°		199.2°	45.7°	12	29.8						
C1 only		64.0°S	79.7°E	11.5°		208.1°	47.8°	7	29.0						*
Component 2															
Site	FM	Slat (°S)	Slong (°E)	Dec (°)	Inc (°)	*n*/*N*	*n*/*C*	*R*	*k*	α_{95}(°)	*s* (°)	λ (°N)	ϕ (°E)	*dp* (°)	*dm* (°)
TCV14	RB	23.1499	147.6045	169.8	1.6	5/5		4.93	43.7	12.8	12.3	−65.5	302.2	6.4	12.8
DBS18	RB	23.4326	147.6259	332.1	−1.8	3/5	1/2	2.97	71.2	14.7	9.6	−54.8	273.4	7.4	14.7
TCV23	RB	23.0946	147.6072	328.7	−8.0	3/5		2.99	26.7	8.7	15.7	−54.2	265.1	4.4	8.8
TCV06	RB	22.9617	147.6006	168.5	−1.2	3/5	1/2	2.98	87.9	13.6	8.64	−63.9	300.6	6.8	13.6
TCV20	RB	23.0101	147.6116	358.2	−10.8	3/5	1/2	2.98	94.9	12.4	8.31	−72.3	321.8	6.4	12.6
DGH	RB	23	147.6	357.2	−5.9	8		7.56	15.9	14.3	20.3	−69.8	320.9	7.2	14.4
TCV-2	TCV	23	147.5	165.9	19.5	9		8.53	17.0	12.9	19.7	−71.3	279.1	7.0	13.5
		λ	ϕ	A_{95}		*D*	*I*	*N*	*k*						*Q*
ChRMs		66.8°S	288.4°	14.7°		345.2°	−8.3°	4	48.7						
All data		66.0°S	290.7°E	9.1°		345.8°	−6.7°	7	36.8						7
Component 3															
Site	FM	Slat (°S)	Slong (°E)	Dec (°)	Inc (°)	*n*/*N*	*n*/*C*	*R*	*k*	α_{95}(°)	*s* (°)	λ (°N)	ϕ (°E)	*dp* (°)	*dm* (°)
DBS01	TCV	22.9243	147.5321	233.9	−71.3	5/5	2/3	4.8	20	17.5	18.1	1.1	354.5	26.8	30.6
DBS12	TCV	22.9245	147.5337	83.4	39.6	3/7	1/2	3.0	101	12.3	8.1	2.9	34.3	8.9	14.8
DBS14	TCV	21.0737	147.5307	87.1	62.9	3/5		2.9	32	22.2	14.3	13.8	14.9	27.3	34.9
TCV01	TCV	22.9086	147.5609	269.6	−53.1	6/7	3/3	5.5	11	21.1	24.4	12.1	25.9	20.3	29.2
TCV02	TCV	22.9122	147.5598	237.2	−57.0	4/5		4.0	135	7.9	7.0	−9.1	10	8.4	10.3
TCV03	TCV	22.9606	147.5457	224.0	−46.6	3/5		3.0	15	19.8	20.9	−23.8	9.7	16.4	25.5
TCV09	TCV	22.9197	147.5556	38.0	67.5	5/5	2/3	4.7	15	20.4	20.9	−9.4	351	28.4	34.0
TCV10	TCV	22.9206	147.5581	17.8	60.1	4/5		3.8	14	25.5	21.6	−24	342.2	29.2	38.6
TCV12	TCV	22.9210	147.5599	250.8	−57.7	4/7		3.9	29	17.4	15.0	0.2	15.4	18.7	25.5
		λ	ϕ	A_{95}		*D*	*I*	*N*	*k*						Q
ChRMs		8.8°N	186.9°E	20.3°		55.0°	59.4°	5	15.2						
All data		4.1°N	188.9°E	14.0°		62.4°	59.5°	9	25.0						6

Component 1 (C1) represents a Middle Carboniferous remagnetization acquired during the Alice Springs Orogeny. Component 2 (C2) reflects a primary thermochemical remanence related to the intrusion and cooling of the Retreat Batholith. Component 3 (C3) is the characteristic component of the Theresa Creek Volcanics at distances greater than 1 km from the TCV/RB contact. Explanation of Table 1 headings: Site, palaeomagnetic site mnemonic; FM is the sampled formation (RB = Retreat Batholith, TCV = Theresa Creek Volcanics); Slat (°S)/Slong (°E) denote latitude/longitude positions for palaeomagnetic sites; Dec (°)/Inc (°) are the declination and inclination in degrees; *n*/*N* is the total number of samples used in analysis compared with the number of samples collected at each palaeomagnetic site; *n*/*C* represents the number of set points/remagnetization circles samples used for analysis, if applicable; *R*, *k*, α_{95}(°), and *s* (°) are calculated Fisher statistics (Fisher 1953) related to mean directions; λ (°N) and ϕ (°E) is the location of the mean palaeopole for each of the site VGPs, *dp*(°)/*dm*(°) correspond to the semi-axes of uncertainty associated with each calculated palaeopole at the 95 per cent confidence level. λ and ϕ in the bottom row of each subsection denote the location of the mean palaeopole calculated from site-level VGPs; A_{95} is the associated half-angle of the 95 per cent confidence cone in degrees; *D*/*I* are the component-level mean declination/inclination calculated from site-level data; N is the number of sites used in calculating each mean; k refers to the precision parameter for components 1–3; *Q* refers to the quality index factor, after Van der Voo (1990). Mean data are presented without and with (ChRM only/All data) GCA data. Also, for C1 data have been presented using both polarities (C1/1′) and the data using only the reverse polarity site means (C1 only), as discussed in the text.

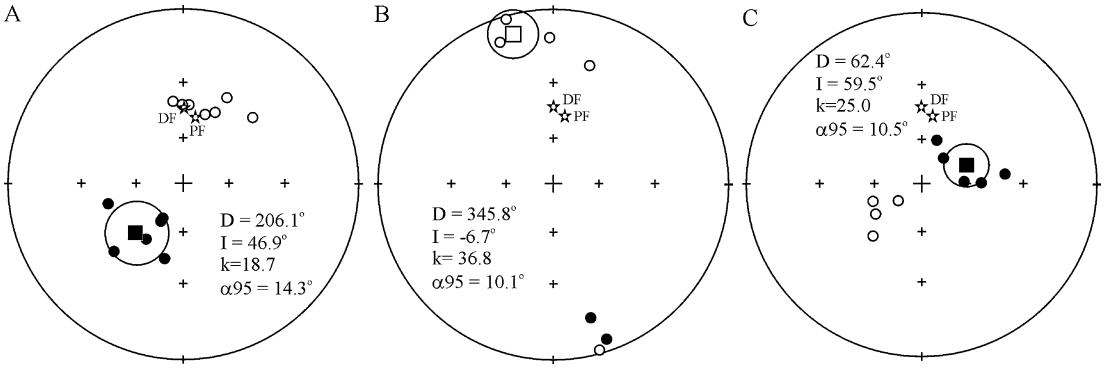

Figure 8. Site-level mean directions of C1 (A), C2 (B) and C3 (C). Stars labelled PF and DF show directions of the present field and the dipole field expected in the sampling region. Squares represent mean directions with associated 95% confidence cones.

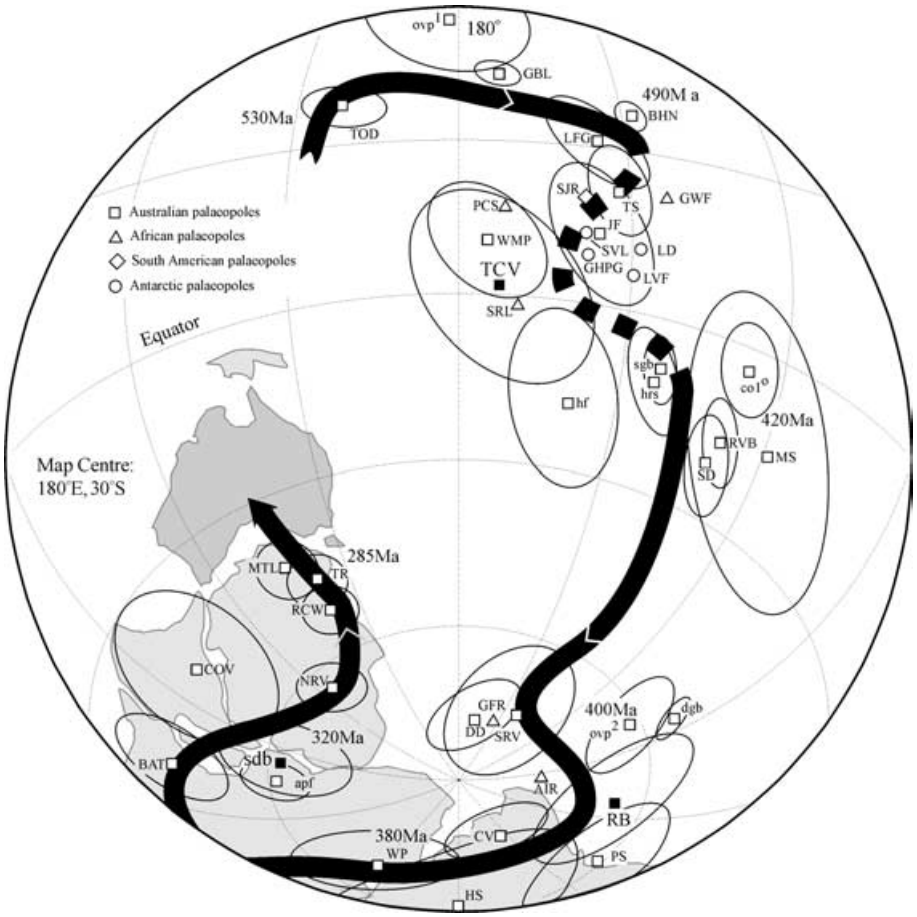

Figure 9. Revised Palaeozoic APWP for Australia. All palaeopoles have been kept in the Australian reference frame. The three palaeomagnetic poles presented herein are marked by filled squares; previously published data are marked by open squares. Triangles, diamonds and circles represent conformable data from Africa, South America and Antarctica, respectively. Data from greater Gondwana have been rotated into the Australian reference frame using the rotation parameters of Lawver & Scotese (1987). Lower case mnemonics refer to palaeopoles that are thought to be magnetically overprinted. Table 2 lists all palaeopole information used for the compilation of this APWP. The plot is an equal-area projection with the map centre located at 30°S, 180°E. Figure modified from GMAP-32 (Torsvik & Smethurst 1989–1997).

recognized, including exhumation within the Mount Isa Block of northern Queensland (Spikings *et al.* 1997) and reactivation of the Darling River Lineament, a segment of the Tasman Line, during the Middle Carboniferous (O'Sullivan *et al.* 1998). Folding took place in the southern Drummond Basin during the ASO, and whilst neither the TCV nor the RB were greatly affected by this deformation (Withnall *et al.* 1995), these units are unlikely to have remained completely impervious to this event. Indeed, it is likely that the normal polarity C1′ direction is pervasive throughout the sampled formations, but its near-coincidence with and partial contamination by a present field or Tertiary magnetization make identification difficult, if not impossible. Possible correlatives with the C1 palaeopole (sdb in Fig. 9) include the Lower Arumbera and Upper Pertataka Formations (apf in Fig. 9; Kirschvink 1978).

Table 2. Palaeopoles used in the revised APWP presented in Fig. 9.

Formation	Pole	Plat (°N)	Plong (°E)	*dp* (°)	*dm* (°)	Age (Ma)	*Q*	GPMDB Ref no./ Reference
Tuckers Range, TFB	TR	−47.5	142	6.0	6.6	280–290	6	A
Mount Leyshon Intrusive Complex, TFB	MTL	−43.2	137.3	6	6.4	280–292	6	A
Rocky Creek and Werrie synclines, TFB	RCW	−53.9	143.7	9	9	306–319	7	3348
Newcastle Range Volcanics, AC	NRV	−63.4	125	6.1	7.9	317–325	6	B
Connors Volcanics, TFB	COV	−46.0	100.0	13.0	16.0	310–330	5	3265
Southern Drummond Basin overprint, TFB	*sdb*	*−64.0*	*79.9*	*9.8*	*15.0*	*320–340*	*	*This study*
L Arumbera & U Pertataka Fm, overprint, AC	apf	−60.2	68.1	4.8	7.1	320–340	*	1070
Bathurst Batholith, TFB	BAT	−45.3	71.9	6.8	10.2	319–332	7	3264
Worange Point Formation, TFB	WP	−67.9	28.6	10.9	10.9	363–367	6	2191
Hermannsburg Sandstone, AC	HS	−61.0	0.9	15.6	15.6	380–385	6	2574
Comerong Volcanics, TFB	CV	−76.9	330.7	7.2	7.2	370–379	6	1565
Parke Siltstone, TFB	PS	−60.9	318.1	7.6	15.1	377–391	6	2574
Retreat Batholith, TFB	*RB*	*−66.0*	*290.7*	*4.6*	*9.1*	*370–390*	*7*	*This study*
Chatsworth & Ninmaroo Fm, overprint, AC	ovp[2]	−61.2	254.1	8.3	10.1	390–410	*	3082
Georgina Basin, Devonian overprint, AC	dgb	−54.9	261.6	2.9	5.8	390–410	*	C
Devonian Dykes, Mount Leyshon, TFB	DD	−78.0	198.8	6.3	9.8	382–415	6	3262
Snowy River Volcanics, TFB	SRV	−74.3	222.7	10.9	14.5	391–417	7	1365
Gilif Hills Ring Complex, Sudan	GFR	−79.3	192.8	19.6	20.6	370–390	5	2189
Aïr Ring Complexes, Niger	AÏR	−83.0	271.8	6.2	6.2	380–400	6	1364
Silurian Dykes, Mount Leyshon, TFB	SD	−21.7	231.9	4.6	8.7	422–428	7	3262
Ravenswood Batholith, TFB	RVB	−17.5	232.7	3.8	7.3	422–428	7	3262
Mereenie Sandstone, AC	MS	−15.7	242.7	23.7	23.7	417–443	5	2574
Chatsworth & Ninmaroo Fm, AC	co1°	−3.1	234.1	7.4	14.8	420–440	*	3082
Georgina Basin, Silurian overprint, AC	sgb	−8.0	216.8	2.6	5.1	420–440	*	C
Hugh River Shale, overprint, AC	hrs	−11.0	217.0	8.5	8.5	420–440	*	210
Hudson Formation, overprint, AC	hf	−18.0	199.0	13.0	13.0	420–440	*	202
Theresa Creek Volcanics, TFB	*TCV*	*4.1*	*188.9*	*15.8*	*21.0*	*435–455*	*6*	*This study*
Salala Ring Complex, Sudan	SRL	−4.1	190.5	8.3	12.3	460–466	6	2715
Walli & Mount Pleasant Andesites, TFB	WMP	12.2	183.3	10.5	15.0	470–495	5	1612
Pakhuis & Cedarberg Fm, South Africa	PCS	18.5	187.5	12.5	21.0	440–460	4	1416
Granit Harbour Pink Granite, East Antarctica	GHPG	14.5	200.6	4.3	8.5	480–500	3	2966
Lake Vanda Feldspar Porphyry Dykes, E Ant.	LVF	9.7	210.1	7.2	7.2	480–500	4	2966
Lamprophyre Dykes, East Antarctica	LD	14.5	212.5	5.5	10.9	470–490	3	1079
South Victoria Land Intrusives, East Antarctica	SVL	11.6	205.9	5.9	5.9	465–485	5	2966
Jinduckin Formation, AC	JF	13.0	205.0	11.0	11.0	485–490	4	202
Salta & Jujuy Redbeds, Argentina	SJR	23.9	206.5	28.5	41.3	470–500	3	613
Tasmanian Sediments, TFB	TS	19.4	208.9	5.3	10.5	500–505	7	3155
Graafwater Fm, South Africa	GWF	22.6	216.9	7.5	11.7	470–495	3	1416
Black Hill Norite, AC	BHN	37.5	214.4	3.2	3.2	485–495	5	2971
Lake Frome Group, overprint, AC	LFG	31.4	206.9	5.1	10.1	490–500	*	1769
Georgina Basin Limestones, AC	GBL	48.6	186.0	2.1	4.0	505–515	7	C
Chatsworth & Ninmaroo Fm, overprint, AC	ovp[1]	57.2	179.3	11.5	22.7	505–515	5	3082
Todd River Dolomite, AC	TOD	43.2	159.9	4.5	7.7	525–535	7	1070

Explanation for Table 2 headings: 'Formation' lists the geological formation from which the data are derived; 'Pole' refers to the palaeopole designators in Fig. 9; Plat (°N)/Plong (°E) mark the location of each presented palaeomagnetic pole; *dp* (°)/*dm* (°) correspond to the semi-axes of uncertainty associated with each calculated palaeopole at the 95 per cent confidence interval; Age (Ma) is the assumed magnetization age for the relevant formation; *Q* describes the quality criteria of Van der Voo (1990) (only those palaeopoles with $Q \geq 4$ were considered for APWP construction); * in *Q* column denotes overprints for which *Q* values were not assigned; GPMDB Ref. No. or Reference correspond to the reference number given in the Global Palaeomagnetic Database (now maintained by Sergei Pisarevsky of the University of Western Australia and available on-line at http://www.geodynamics.no/) or the journal reference of data not yet assigned a reference number in the database (A, Clark & Lackie (2003); B, Anderson *et al.* (2003); C, Anderson *et al.* (2004)). Gondwana data were rotated into the Australian reference frame using the rotation parameters of Lawver & Scotese (1987). Lower cased italicized mnemonics represent data that are thought to be palaeomagnetically overprinted. Italicized entries are data presented from this study. For Australian data, AC and TFB refer to palaeopoles obtained from cratonic Australia and the Palaeozoic Tasman Fold Belt, respectively.

A contact test between the RB and TCV demonstrated that C3 is found only within the TCV and only at distances greater than 1 km from the TCV/RB contact. Palaeomagnetic results also showed that C2, the ChRM associated with the batholith, is found in samples taken from the TCV/RB contact zone and is interpreted to be a thermal remagnetization (haematite) of the TCV. The isolation of the C3 component within the TCV and the presence of C2 only within the hornfelsed volcanics argue for a positive outcome for the contact test and a stable magnetization of the TCV at least since the time of the intrusion of the RB. The disparate directions characterizing these two formations strongly support a pre-Middle Devonian age, and probably a much older age, for the TCV.

Polarity ambiguities and a lack of reliable palaeomagnetic data for the Late Ordovician–Early Silurian seriously inhibit attempts to construct a robust Early Palaeozoic APWP for Gondwana (e.g. Li & Powell 2001). This uncertainty also complicates attempts to date

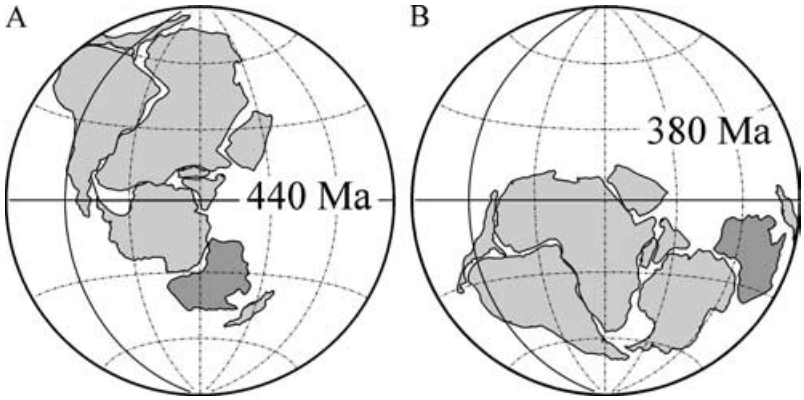

Figure 10. Palaeozoic reconstructions for Gondwana based upon the ∼440 Ma Theresa Creek Volcanics (A) palaeopole and the ∼380 Ma Retreat Batholith (B) pole.

the TCV palaeomagnetically. However, using the rotation parameters of Lawver & Scotese (1987), several Gondwanan palaeopoles agree with the TCV pole when rotated into Australian coordinates (Fig. 9 and Table 2). Spatial and temporal consistency between the TCV palaeopole with these Gondwanan poles is compatible with an assumed Late Ordovician age for the TCV based upon chemical similarity with the Bolindian Fork Lagoons Beds and the pre-Middle Devonian magnetization age defined by the contact test between the RB and TCV.

In generation of the Early Palaeozoic segment of the pole path presented in Fig. 9, the 'polarity option' was invoked for pre-Silurian palaeopoles. The alternate polarity option for Early Palaeozoic poles was first proposed by Schmidt & Morris (1977) to account for seemingly anomalous palaeopoles from the Tasman Fold Belt of eastern Australia and has since been utilized by Li *et al.* (1991), Rapalini & Vilas (1991) and Clark & Lackie (2003). In this scheme, palaeomagnetic directions from some Cambrian formations in Western Australia and the Northern Territory, in particular the Hudson Formation (Luck 1972) and Hugh River Shales (Embleton 1972) (hf and hrs in Fig. 9) are taken to reflect Late Ordovician–Early Silurian remagnetizations. As the magnetization ages of these formations are essentially unconstrained by either field or stability tests and the palaeopoles fall closer to the 490–430 Ma segment of the pole path than to well-constrained Cambrian palaeopoles, remagnetization seems a likely possibility.

The dashed segment of the presented APWP between the ∼490 Ma Black Hill Norite (BHN) (Schmidt *et al.* 1993) and that of the ∼420 Ma Mount Leyshon Silurian Dykes (SD) (Clark 1996) poles incorporates these possible remagnetizations and the assumed Late Ordovician age for the TCV. A similar excursion is documented in the conventional polarity pole path presented by Li & Powell (2001). Until such a time that the TCV are radiometrically dated or reliable Late Ordovician–Early Silurian Australian data are available, however, this excursion can only be tentatively incorporated into Australia's APWP.

Apparent polar wander paths are characteristically represented as long arcs joined by the occasional cusp or (more rarely) hairpin, indicative of orogenesis and/or plate reorganization. Generation of such APWPs is usually the result of compilation studies and the averaging of palaeopoles from an inventory of similarly aged, similarly positioned palaeopoles (e.g. Van der Voo 1993; Li & Powell 2001). Whereas such endeavours are invaluable in tracing the large-scale tectonic history of a continent, or indeed all major plates, the very nature of such studies precludes attention to detail, eschewing hairpin swings in a continent's APWP in favour of overall conformity. APWPs constructed in this manner have the potential to be unrealistically shortened and drift velocities artificially lowered. In contrast to this, the APWP presented in Fig. 9 incorporates a Late Ordovician–Early Silurian 'excursion' into the pole path and a set of Early Devonian hairpins that lengthen the pole path and increase drift velocities for much of the Palaeozoic. Invoking alternate polarities for pre-Silurian data makes both the Ravenswood Batholith data (Clark 1996) and that from the Drummond Basin conformable with Australia's Early Palaeozoic APWP without applying of a 90° tectonic rotation to most of Queensland, such as was recently proposed by McElhinny *et al.* (2002). The alternate polarity scheme also allows for incorporation of data without drift velocities of 60 cm yr^{-1}, as required by the Morel & Irving (1978) APWP model and its subsequent derivatives. It is preferable at this juncture to allow conformity of the available palaeomagnetic data over tectonic disruption of cratonized elements of Queensland and/or drift rates that cannot be geodynamically corroborated.

A series of Late Ordovician–Early Devonian reconstructions for Gondwana are provided in Fig. 10. The high-latitude position of northwest Africa in Fig. 10(a) (terminal Ordovician reconstruction) is in keeping with the presence of glaciogenic sequences in this area during this period (e.g. Ghienne 2003). Australia remains at low latitudes between the ∼450 Ma and 420 Ma reconstructions, compatible with the presence of Late Ordovician–Silurian evaporates found throughout northern Australia. The last image, Fig. 10(c), based upon the RB palaeopole, documents the migration of West Gondwana back into polar latitudes prior to the Late Devonian glaciation (Caputo 1985).

6 CONCLUSIONS

Three new palaeomagnetic poles are presented as a part of this study. The sdb pole (64.0°S, 79.7°E, $N = 7$, $A_{95} = 11.5°$) is thought to reflect a remagnetization related to the Middle Carboniferous (∼340–320 Ma) ASO. Deformation throughout Australia, related to the ASO, has been documented and it is suggested that remagnetizations related to this event may be more widespread than previously thought.

While the RB pole (66.0°S, 290.7°E, $N = 7$, $A_{95} = 9.1°$) adds little information to the well-defined Devonian section of the pole path, its agreement with similarly aged poles, the age constraint of the contact test and palaeomagnetic statistics related to this pole

make it one of high quality ($Q = 7$) and, therefore, suitable for anchoring the APWP during this period.

At distances greater than 1 km from the contact between the TCV and the intruding RB, the TCV provides a palaeopole at 4.1°N, 188.9°E ($N = 9$, $A_{95} = 14.0°$). Although this formation lacks a definitive radiometric age, the related palaeopole is consistent with the Late Ordovician–Early Silurian segment of Australia's APWP and agrees with similarly aged palaeopoles from greater Gondwana. The presence of the Late Ordovician Fork Lagoons Beds to the south of the TCV supports this age assignment, as geochemical data suggest these two units may be cogenetic (Fig. 5).

ACKNOWLEDGMENTS

The authors would like to thank P. Schmidt, M. McElhinny and C. Klootwijk for their reviews of this paper and C. Langereis in his role as GJI editor as their respective critiques have resulted in a greatly improved manuscript. We also would like to acknowledge P. Blake and I. Withnall of the Queensland Department of Minerals and Energy and J. Talent of MUCEP (Macquarie University) for discussions related to the structure of the southern Drummond and S. Touron and N. Peterson of GEMOC (Macquarie University) for assistance with the geochemistry. KLA would personally like to extend thanks to station owners for access to their properties and C. Anderson Justice and G. Justice for assistance in the field. This work was funded in part by two Macquarie University Post-Graduate Research Fund awards. This is publication 324 in the GEMOC National Key Centre.

REFERENCES

Anderson, K.L., Lackie, M.A., Clark, D.A. & Schmidt, P.W., 2003. Paleomagnetism of the Newcastle Range, northern Queensland: eastern Gondwana in the Late Paleozoic, *J. geophys. Res.,* **108**(B6), 2282–2282.

Anderson, K.L., Lackie, M.A., Clark, D.A. & Schmidt, P.W., 2004. Return to Black Mountain: palaeomagnetic reassessment of the Chatsworth and Ninmaroo formations, western Queensland, Australia, *Geophys. J. Int.,* **157**(1), 87–104, doi:10.1111/j.1365-246X.2003.02164.x.

Butler, R.F., 1992. *Paleomagnetism: Magnetic Domains to Geologic Terranes,* Blackwell, Boston, MA.

Caputo, M.V., 1985. Late Devonian glaciation in South America, *Palaeogeogr. Palaeoclim. Palaeoecol.,* **51,** 291–317.

Chen, Z., Li, Z.X., Powell, C.McA. & Balme, B.E., 1993. Palaeomagnetism of the Brewer Conglomerate in central Australia, and fast movement of Gondwanaland during the Late Devonian, *Geophys. J. Int.,* **115,** 564–574.

Clark, D.A., 1996. *Palaeomagnetism of the Mount Leyshon Intrusive Complex, the Tuckers Range Igneous Complex and the Ravenswood Batholith,* CSIRO Exploration and Mining Report, 318R, CSIRO Division of Exploration and Mining, Sydney.

Clark, D.A. & Lackie, M.A., 2003. Palaeomagnetism of the Early Permian Mount Leyshon Intrusive Complex and Tuckers Igneous Complex, north Queensland, Australia, *Geophys. J. Int.,* **153,** 523–547.

Cook, P.J. & Totterdel, J.M., 1991. *Palaeogeographic Atlas of Australia, Volume 2, Ordovician,* Australia Bureau of Mineral Resources, Geology & Geophysics, Canberra.

Davis, B.K. & Henderson, R.A., 1996. Rift-phase extensional fabrics of the back-arc Drummond Basin, eastern Australia, *Basin Res.,* **8,** 371–381.

Day, R., Fuller, M.D. & Schmidt, V.A., 1977. Hysteresis properties of titanomagnetites: grain size and composition difference, *Phys. Earth planet. Int.,* **13,** 260–267.

Deo, S.D., 1991. Geology and geochemistry of the Theresa Creek area, central Queensland, *Postgraduate Diploma in Science Thesis,* University of Queensland, Brisbane.

Dunlop, D.J. & Özdemir, Ö., 1997. *Rock Magnetism: Fundamentals and Frontiers,* Cambridge University Press, Cambridge.

Embleton, B.J.J., 1972. The palaeomagnetism of some Proterozoic-Cambrian sediments from the Amadeus Basin, Central Australia, *Earth planet. Sci. Lett.,* **17,** 217–226.

Everitt, C.W.F. & Clegg, J.A., 1962. A field test for palaeomagnetic stability, *Geophys. J. R. astr. Soc.,* **6,** 312–319.

Fisher, R.A., 1953. Dispersion on a sphere, *Proc. R. Soc. Lond.,* A., **217,** 295–305.

Ghienne, J.-F., 2003. Late Ordovician sedimentary environments, glacial cycles, and post-glacial transgression in the Taoudeni Basin, West Africa, *Palaeogeogr. Palaeoclim. Palaeoecol.,* **189,** 119–145.

Kirschvink, J.L., 1978. The Precambrian–Cambrian boundary problem: paleomagnetic directions from the Amadeus Basin, Central Australia, *Earth planet. Sci. Lett.,* **40,** 91–100.

Kirschvink, J.L., 1980. The least-squares line and plane and the analysis of palaeomagnetic data, *Geophys. J. R. astr. Soc.,* **62,** 699–718.

Klootwijk, C., Giddings, J.W. & Percival, P., 1993. *Palaeomagnetic Reconnaissance of Upper Palaeozoic Volcanics, Northeastern Queensland,* Australian Geological Survey Organisation Record 1993/36, Australian Geological Survey, Canberra.

Lawver, L.A. & Scotese, C.R., 1987. A revised reconstruction of Gondwanaland, in *Gondwana Six; Structure, Tectonics, and Geophysics,* American Geophysical Union Monograph 40, pp. 17–23, ed. McKenzie, G.D., American Geophysical Union, Washington, DC.

Li, Z.X. & Powell, C.McA., 2001. An outline of the palaeogeographic evolution of the Australasian region since the beginning of the Neoproterozoic, *Earth Sci. Rev.,* **53,** 237–277.

Li, Z.X., Powell, C.McA., Embleton, B.J.J. & Schmidt, P.W., 1991. New palaeomagnetic results from the Amadeus Basin and their implications for stratigraphy and tectonics, *Aust. Bur. Min. Res. Bull.,* **236,** 349–360.

Lowrie, W., 1990. Identification of ferromagnetic minerals in a rock by coercivity and unblocking temperature properties, *Geophys. Res. Lett.,* **17,** 159–162.

Luck, G.R., 1972. Palaeomagnetic results from Palaeozoic sediments of Northern Australia, *Geophys. J. Roy. astr. Soc.,* **28,** 475–487.

McDonough, W.F. & Sun, S.-S., 1995. The composition of the Earth, *Chem. Geol.,* **120,** 223–253.

McElhinny, M.W. & McFadden, P.L., 2000. *Paleomagnetism Continents and Oceans,* Academic Press, San Diego, CA.

McElhinny, M.W., Powell, C.McA. & Pisarevsky, S.A., 2002. Paleozoic terranes of eastern Australia and the drift history of Gondwana, *Tectonophysics,* **362,** 41–65.

McFadden, P.L. & McElhinny, M.W., 1988. The combined analysis of remagnetization circles and direct observations in palaeomagnetism, *Earth planet. Sci. Lett.,* **87,** 161–172.

Morel, P. & Irving, E., 1978. Tentative palaeocontinental maps for the Early Phanerozoic and Proterozoic, *J. Geol.,* **86,** 535–561.

O'Sullivan, P.B., Kohn, B.P. & Mitchell, M.M., 1998. Phanerozoic reactivation along a fundamental Proterozoic crustal fault, the Darling River Lineament, Australia; constraints from apatite fission track thermochronology, *Earth planet. Sci. Lett.,* **164,** 451–465.

Powell, C.McA., 1984. Terminal fold-belt deformation: relationship of mid-Carboniferous megakinks in the Tasman fold belt to coeval thrusts in cratonic Australia, *Geology,* **12,** 546–549.

Rapalini, A.E. & Vilas, J.F., 1991. Preliminary paleomagnetic data from the Sierra Grande Formation: tectonic consequences of the first mid-Paleozoic paleopoles from Patagonia, *J. S. Am. Earth Sci.,* **4,** 25–41.

Schmidt, P.W., 1985. Bias in converging great circle methods, *Earth planet. Sci. Lett.,* **72,** 427–432.

Schmidt, P.W., 1993. Palaeomagnetic cleaning strategies, *Phys. Earth planet. Int.,* **76,** 169–178.

Schmidt, P.W. & Embleton, B.J.J., 1990. The palaeomagnetism of the Tumblagooda Sandstone, Western Australia: Gondwana Palaeozoic apparent polar wandering, *Phys. Earth planet. Int.,* **64,** 303–313.

Schmidt, P.W. & Morris, W.A., 1977. An alternative view of the Gondwana Paleozoic apparent polar wander path, *Can. J. Earth Sci.,* **14,** 2674–2678.

Schmidt, P.W., Embleton, B.J.J. & Palmer, H.C., 1987. Pre and post folding magnetization from the Devonian Snowy River Volcanics and Buchan Caves Limestone, Victoria, *Geophys. J. R. astr. Soc.,* **91,** 155–170.

Schmidt, P.W., Clark, D.A. & Rajagopalan, S., 1993. An historical perspective of the Early Palaeozoic APWP of Gondwana: new results from the Early Ordovician Black Hill Norite, South Australia, *Expl. Geophys.,* **24,** 257–262.

Spikings, R.A., Foster, D.A. & Kohn, B.P., 1997. Phanerozoic denudation history of the Mt Isa Inlier, northern Australia; response of a Proterozoic mobile belt to intraplate tectonics, *Int. Geol. Rev.,* **39,** 107–124.

Tauxe, L., 1998. *Paleomagnetic Principles and Practice,* Kluwer Academic Publishers, Dordrecht.

Thrupp, G.A., Kent, D.B., Schmidt, P.W. & Powell, C.McA., 1991. Paleomagnetism of red beds of the Late Devonian Worange Point Formation, SE Australia, *Geophys. J. Int.,* **104,** 179–201.

Torsvik, T.H. & Rehnström, E.F., 2001. Cambrian palaeomagnetic data from Baltica; implications for true polar wander and Cambrian palaeogeography, *J. geol. Soc. Lond.,* **158,** 321–329.

Torsvik, T. & Smethurst, M., 1989. *GMAP-32, Geographic Mapping and Reconstruction System,* Geological Survey of Norway, Trondheim.

Van der Voo, R., 1990. The reliability of palaeomagnetic poles, *Tectonophysics,* **184,** 1–9.

Van der Voo, R., 1993. *Paleomagnetism of the Atlantic, Tethys, and Iapetus Oceans,* Cambridge University Press, Cambridge.

Veevers, J.J., Jones, J.B. & Powell, C.McA., 1982. Tectonic framework of Australia's sedimentary basins, *Aust. Petrol. Expl. Assoc. J.,* **22,** 283–300.

Withnall, I.W. *et al.,* 1995. Geology of the southern part of the Anakie Inlier, central Queensland, *Queensland Geol.,* 7.

Zijderveld, J.D.A., 1967. A.C. demagnetization of rocks: analysis of results, in *Methods in Palaeomagnetism,* pp. 254–286, eds Collinson, D.W., Creer, K.M. & Runcorn, S.K., Elsevier, New York.